PERTURBATION ESTIMATION BASED ROBUST PASSIVE CONTROL OF PERMANENT MAGNETIC SYNCHRONOUS GENERATOR FOR OPTIMAL POWER EXTRACTION

Bo Yang[1], Yiyan Sang[2], Lin Jiang[2], Tao Yu[3]

[1] Faculty of Electric Power Engineering, Kunming University of Science and Technology, 650500 Kunming, China
[2] Department of Electrical Engineering & Electronics, University of Liverpool, Liverpool, L69 3GJ, United Kingdom
[3] College of Electric Power, South China University of Technology, 510640 Guangzhou, China
Corresponding author: Lin Jiang, e-mail: l.jiang@liverpool.ac.uk

REFERENCE NO	ABSTRACT
MISC-01	This paper designs a perturbation estimation based robust passive control (PERPC) scheme of permanent magnetic synchronous generator (PMSG) to achieve optimal power extraction. The generator nonlinearities, parameter uncertainties, and unmodelled dynamics are aggregated into a perturbation which is then estimated in the real-time by a high-gain state and perturbation observer (HGSPO). Then, the estimated perturbation is fully compensated by a passive controller, such that a considerable robustness and improved system damping can be simultaneously realized. Case studies including step change of wind speed, random wind speed variation, and generator parameter uncertainties have been undertaken. Simulation results verify the effectiveness and superiority of PERPC compared to that of conventional vector control (VC) and feedback linearization control (FLC).
Keywords: PMSG, optimal power extraction, perturbation observer, robust passive control, wind energy conversion system	

Nomenclature

	Variables		*Abbreviations*
v_{wind}	wind velocity	MPPT	maximum power point tracking
ρ	air density	PMSG	permanent magnetic synchronous generator
C_P	power coefficient	VC	vector control
λ	tip-speed-ratio	HGSPO	high-gain state and perturbation observer
β	blade pitch angle	HGPO	high-gain perturbation observer
T_e	electromagnetic torque	SPWM	sinusoidal pulse width modulation
T_m	mechanical torque	VSC	voltage source converter
ω_e	electrical rotation speed	PID	proportional-integral-derivative
ω_m	mechanical rotation speed of turbine	FLC	feedback linearization control
V_d, V_q	dq-axis stator voltages	PERPC	perturbation estimation based robust passive control
i_d, i_q	dq-axis currents	WECS	Wind energy conversion system
	System parameters		*The control parameters of PERPC*
L_d, L_q	dq-axis inductances	λ_1, λ_2	energy shaping coefficients
p	the number of pole pairs	α_i	Luenberger observer gains
R	turbine radius	k_{11}, k_{21}, k_{22}	control gains
J_{tot}	total inertia of the drive train	v_1, v_2	additional control inputs
D	viscous damping coefficient	ϵ_1, ϵ_2	thickness layer boundary of observer
R_s	stator resistance	B_0	constant control gain

1. INTRODUCTION

The fast depletion of conventional fossil fuels (coal, gas, oil) and ever-growing population around the globe have driven the modern power industry to exploit the renewable energy, e.g., wind, solar, biomass, tidal, geothermal, etc.[1]. Among which wind energy conversion system (WECS) is one of the most widely used sustainable energy form thanks to the abundance and cleanness of wind in nature [2].

Currently, there are mainly two types of wind generators, i.e., doubly-fed induction generator (DFIG) [3] and permanent magnetic synchronous generator (PMSG) [4]. In the past decade, PMSG has gained considerable attentions in both industry and academics thanks to its simple structure and gearless construction. At the moment, one of the major tasks of PMSG control system design is to optimally extract the wind energy under various wind profiles, also called maximum power point tracking (MPPT), such that high energy conversion efficiency could be realized.

Conventional vector control (VC) incorporated with proportional-integral-derivative (PID) loops are widely employed for PMSG due to its easy implementation and high reliability [5]. However, its control performance may undesirably degrade or even result in a system stability collapse when operation conditions vary significantly as its control parameters are determined through the one-point linearization model of the original PMSG system, which is however highly nonlinear due to the converter dynamics and often operate in a large range caused by the stochastic wind speed, hence the MPPT performance of VC is generally not optimal.

In order to handle the above challenge, plenty of advanced approaches have been proposed. In reference [6], a feedback linearization control (FLC) was designed to fully compensate the PMSG nonlinearities, such that a globally consistent control performance can be achieved. However, it requires an accurate system model which is however impossible in practice. Thus, several robust/adaptive control strategies have been investigated to remedy such shortcomings. An enhanced exponential reaching law based sliding-mode control (SMC) was devised for PMSG to enhance total harmonic distortion property with improved robustness against to parameter uncertainties [7]. Furthermore, a robust nonlinear predictive control (RNPC) was reported in [8] to simultaneously achieve MPPT and battery charging regardless of the presence of disturbances. Besides, a model predictive control (MPC) and dead-beat predictive control strategies were employed to forecast the possible future behaviour of the control variables of PMSG, such that a more optimal control performance can be achieved, together with enhanced robustness against to modelling uncertainties [9]. In addition, reference [10] developed a nonlinear Luenberger-like observer which aims to estimate the mechanical variables by only the measurement of electrical variables of PMSG for MPPT. Meanwhile, an active disturbance rejection control (ADRC) was developed to fully compensate the lumped disturbances in the real-time thus MPPT could be achieved [11].

Nevertheless, the aforementioned approaches merely regard the PMSG control as a pure mathematical problem while its physical meaning/nature is somehow ignored.

Passivity provides a power tool to analyse the essential physical property of a given engineering problem by carefully examining the storage function of the controlled system, upon energy reshaping, to improve the system damping [12]. Based on passivity theory, an interconnection and damping assignment passivity-based control (IDA-PBC) scheme was proposed in [13] to achieve a satisfactory MPPT of PMSG under severe wind speed variations. However, such strategy still needs an accurate system model. To handle this issue, an adaptive passivity-based control (APBC) [14] was applied, which employs a wind speed estimator to enhance the robustness of the PMSG system in the presence of uncertain generator parameters.

Thus far, how to effectively and efficiently handle various types of uncertainties of PMSG system with the exploitation of PBC still remains challenging. Hence, this paper attempts to propose a perturbation estimation based robust passive control (PERPC) scheme to resolve such obstacle by the use of a linear perturbation observer (PO) called high-gain state and perturbation observer (HGSPO) [15,16]. Under such framework, the PMSG nonlinearities, parameter uncertainties, and unmodelled dynamics are aggregated into a perturbation which is rapidly estimated by HGSPO in the real-time. Then, the estimated perturbation is fully compensated by a passive controller to accomplish a robust passive control strategy, which can therefore own the damping enhancement of PBC and robustness improvement of PO based control simultaneously. Three case studies are undertaken, including step change of wind speed, random wind speed variation, and generator parameter uncertainties. Simulation results verify the effectiveness of PERPC.

The remaining of this paper is organized as follows: Section 2 develops the PMSG model. Section 3 is devoted to present the PERPC, which is applied on PMSG for MPPT in Section 4. In Section 5, case studies are carried out while Section 6 concludes the paper with some remarkable contributions.

2. PMSG MODELLING

The configuration of PMSG based WECS is illustrated by Fig. 1. Here, the generator-side VSC attempts to realize MPPT via adjusting

the mechanical rotation speed. As this paper focuses on the MPPT of PMSG, the grid-side VSC modelling is ignored.

The wind turbine model can be described by a power coefficient $C_p(\lambda, \beta)$, which is usually an algebraic function of both blade pitch angle β and tip-speed-ratio λ, with λ being defined by [17,18]

$$\lambda = \frac{\omega_m R}{v_{wind}} \quad (1)$$

where ω_m denotes the mechanical rotation speed of wind turbine and v_{wind} represents the wind speed; and R represents the blade radius of wind turbine, respectively. A generic equation employed to describe the power coefficient $C_p(\lambda, \beta)$ can be usually written as

$$C_p(\lambda, \beta) = c_1 \left(\frac{c_2}{\lambda_i} - c_3\beta - c_4 \right) e^{-\frac{c_5}{\lambda_i}} \quad (2)$$

with

$$\frac{1}{\lambda_i} = \frac{1}{\lambda + 0.08\beta} - \frac{0.035}{\beta^3 + 1} \quad (3)$$

where the coefficients c_1 to c_5 are chosen as c_1=0.22, c_2=116, c_3=0.4, c_4=5, and c_5=12.5, respectively [17,18].

In addition, the mechanical power extracted by the wind turbine from the wind energy is obtained as

$$P_m = \frac{1}{2}\rho\pi R^2 C_p(\lambda, \beta) v_{wind}^3 \quad (4)$$

where ρ denotes the air density. Note that during MPPT the wind turbine only operates in the sub-rated speed range hence its pitch control is deactivated for the whole operation of PMSG.

The dynamics of PMSG in the d-q reference frames are written as [17,18]

$$V_d = i_d R_s + L_d \frac{di_d}{dt} - \omega_e L_q i_q \quad (5)$$

$$V_q = i_q R_s + L_q \frac{di_q}{dt} + \omega_e (L_d i_d + K_e) \quad (6)$$

$$T_e = p[(L_d - L_q)i_d i_q + i_q K_e] \quad (7)$$

where V_d and V_q represent the d-q axis stator voltages; i_d and i_q denote the d-q axis currents; L_d and L_q mean the d-q axis inductances; electrical rotation speed $\omega_e = p\omega_m$; K_e is the permanent magnetic flux of magnets; R_s is the stator resistance; and p is the number of pole pairs, respectively.

The dynamics of mechanical shaft system and mechanical torque of PMSG are given by

$$J_{tot}\frac{d\omega_m}{dt} = T_m - T_e - D\omega_m \quad (8)$$

$$T_m = \frac{1}{2}\rho\pi R^5 \frac{C_p(\lambda, \beta)}{\lambda^3}\omega_m^2 \quad (9)$$

where J_{tot} represents the total inertia of the drive train which lumps the generator inertia and wind turbine inertia; the viscous damping coefficient D=0; and T_m denotes the mechanical torque of the wind turbine, respectively. In addition, active power is calculated as

$$P_e = T_e \omega_e \quad (10)$$

where T_e represents the electromagnetic torque.

In order to achieve MPPT, the power coefficient $C_p(\lambda, \beta)$ should be maintained at its maximum point C_p^* at various wind speed. Here, the pitch angle is taken as $\beta = 2°$, the optimal tip-speed-ratio $\lambda^* = 7.4$ while maximum power coefficient $C_p^* = 0.4019$ [17,18].
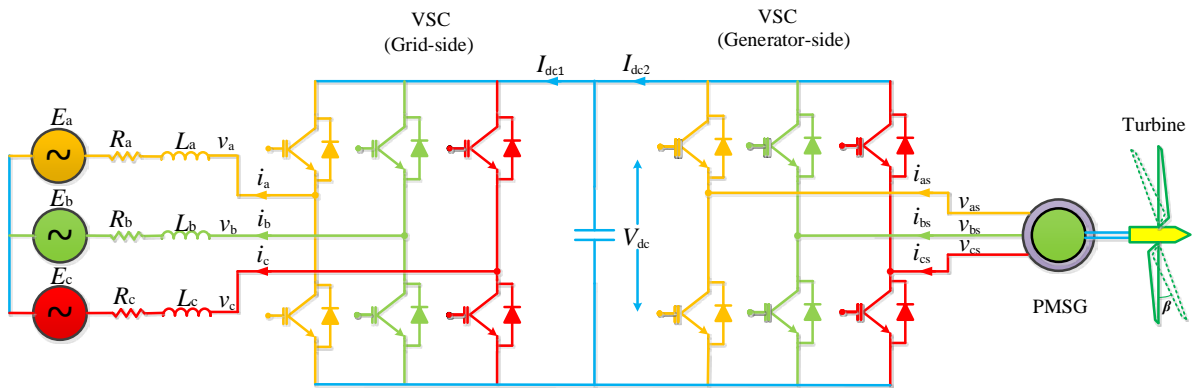

Fig. 1. Configuration of a PMSG based WECS.

3. METHODOLOGY

Consider an uncertain nonlinear system which has the following canonical form

$$\begin{cases} \dot{x} = Ax + B(a(x) + b(x)u + d(t)) \\ \qquad\qquad y = x_1 \end{cases} \quad (11)$$

where $x = [x_1, x_2, \cdots, x_n]^T \in R^n$ is the state variable vector; $u \in R$ and $y \in R$ are the control input and system output, respectively; $a(x): R^n \mapsto R$ and $b(x): R^n \mapsto R$ are unknown smooth functions; and $d(t): R^+ \mapsto R$ represents a time-varying external disturbance. The $n \times n$ matrix A and $i \times i$ matrix B are of the canonical form as follows

$$A = \begin{bmatrix} 0 & 1 & 0 & L & 0 \\ 0 & 0 & 1 & L & 0 \\ M & M & M & M & M \\ 0 & 0 & 0 & L & 1 \\ 0 & 0 & 0 & L & 0 \end{bmatrix}_{n \times n}, B = \begin{bmatrix} 0 \\ 0 \\ M \\ 0 \\ 1 \end{bmatrix}_{n \times 1} \quad (12)$$

The perturbation of system (1) is defined as [1,3,15,16]

$$\psi(x, u, t) = a(x) + (b(x) - b_0)u + d(t) \quad (13)$$

where b_0 is the constant control gain.

From the original system (11), the last state x_n can be rewritten in the presence of perturbation (13), gives

$$\dot{x}_n = a(x) + (b(x) - b_0)u + d(t) + b_0 u = \psi(x, u, t) + b_0 u \quad (14)$$

Define a ficticious state (extended state) $x_{n+1} = \psi(x, u, t)$. Then, system (11) can be directly extended into

$$\begin{cases} \qquad y = x_1 \\ \quad \dot{x}_1 = x_2 \\ \qquad \vdots \\ \dot{x}_n = x_{n+1} + b_0 u \\ \dot{x}_{n+1} = \dot{\psi}(\cdot) \end{cases} \quad (15)$$

The new state vector can be rewritten as $x_e = [x_1, x_2, \cdots, x_n, x_{n+1}]^T$, together with the following two assumptions being made [15,16]

A.1 b_0 is chosen to satisfy $|b(x)/b_0 - 1| \leq \theta < 1$, where θ is a positive constant.

A.2 The function $\psi(x, u, t): R^n \times R \times R^+ \mapsto R$ and $\dot{\psi}(x, u, t): R^n \times R \times R^+ \mapsto R$ are bounded over the domain of interest $|\psi(x, u, t)| \leq r_1, |\dot{\psi}(x, u, t)| \leq r_2$ with $\psi(0, 0, 0) = 0$ and $\dot{\psi}(0, 0, 0) = 0$, where γ_1 and γ_2 are positive constants.

Throughout this paper, $\tilde{x} = x - \hat{x}$ refers to the estimation error of x whereas $\hat{x}$ represents the estimate of x, while x^* denotes the reference of x. Consider the worst case, e.g., $y = x_1$ is the only

measurable state, an $(n+1)$th-order HGSPO for the extended system (15) is used to simultaneously estimate all unmeasurable states and perturbation, as follows [15,16]

$$\dot{\hat{x}}_e = A_0 \hat{x}_e + B_1 u + H(x_1 - \hat{x}_1) \quad (16)$$

where $H = [\alpha_1/\varepsilon, \alpha_2/\varepsilon^2, \ldots, \alpha_n/\varepsilon^n, \alpha_{n+1}/\varepsilon^{n+1}]^T$ is the observer gain; $0 \leq \varepsilon \leq 1$ represents the thickness layer boundary of HGSPO; and Luenberger observer gains α_i, $i = 1, 2, \cdots, n+1$, are chosen to allocate the poles of polynomial $s_{n+1} + \alpha_1 s_n + \alpha_2 s_{n-1} + \cdots + \alpha_{n+1} = (s + \lambda_\alpha)^{n+1} = 0$ being in the open left-half complex plane at $-\lambda_\alpha$, with

$$\alpha_i = C_{n+1}^i \lambda_\alpha^i, i = 1, 2, \cdots, n + 1. \quad (17)$$

Apply the estimate of states and perturbation, the PERPC for the original system (11) is designed as

$$\begin{cases} u = b_0^{-1}\left(-\hat{\psi}(\cdot) - K(\hat{x} - x^*) + v\right) \\ \qquad\qquad v = -\phi(y) \end{cases} \quad (18)$$

where v is an additional input; $\phi(y)$ is any smooth function satisfying $\phi(0) = 0$ and $y\phi(y) > 0$ for all $y \neq 0$, such that the closed-loop system can be transformed into output strictly passive system [12]; and $K = [k_1, k_2, \cdots, k_n]$ is the feedback control gain, which makes matrix $A_1 = A - BK$ Hurwitzian.

4. PERPC DESIGN FOR PMSG

Define the tracking error $e = [e_1, e_2]^T = [i_d - i_d^*, \omega_m - \omega_m^*]^T$, with i_d^* and ω_m^* being the references of d-axis current and mechanical rotation speed, respectively. Differentiate the tracking error until the control input $u = [u_1, u_2]^T = [V_d, V_q]^T$ appears explicitly, yields

$$\begin{bmatrix} \dot{e}_1 \\ \ddot{e}_2 \end{bmatrix} = \begin{bmatrix} f_1(\cdot) \\ f_2(\cdot) \end{bmatrix} + B \begin{bmatrix} u_1 \\ u_2 \end{bmatrix} - \begin{bmatrix} \dot{i}_d^* \\ \ddot{\omega}_m^* \end{bmatrix} \quad (19)$$

where

$$f_1(x) = -\frac{R_s}{L_d}i_d + \frac{\omega_e L_q}{L_d}i_q \quad (20)$$

$$f_2(x) = \frac{\dot{T}_m}{J_{tot}} - \frac{p i_q}{J_{tot}L_q}(L_d - L_q)(-R_s i_d + L_q \omega_e i_q) + \frac{p}{J_{tot}L_q}[K_e + (L_d - L_q)i_d](L_d \omega_e i_d + R_s i_q + \omega_e K_e) \quad (21)$$

with

$$B(x) = \begin{bmatrix} \frac{1}{L_d} & 0 \\ -\frac{p i_q}{J_{tot}L_d}(L_d - L_q) & -\frac{p}{J_{tot}L_q}[K_e + (L_d - L_q)i_d] \end{bmatrix} \quad (22)$$

The inverse of control gain matrix $B(x)$ can be calculated, as follows

$$B^{-1}(x) = \begin{bmatrix} L_d & 0 \\ -\frac{i_q L_q(L_d - L_q)}{K_e + (L_d - L_q)i_d} & -\frac{J_{tot}L_q}{p[K_e + (L_d - L_q)i_d]} \end{bmatrix} \quad (23)$$

In order to ensure the above input-output line arization to be valid, control gain matrix $B(x)$ is re quired to be nonsingular among the whole operati on range of PMSG, it obtains

$$\det[B(x)] = -\frac{p[K_e + (L_d - L_q)i_d]}{J_{tot}L_d L_q} \neq 0 \quad (24)$$

which can be always satisfied when $K_e \neq -(L_d - L_q)i_d$.

Assume all generator nonlinearities and parameters are uncertain, define the perturbations $\psi_1(\cdot)$ and $\psi_2(\cdot)$ for system (19) as

$$\begin{bmatrix} \psi_1(\cdot) \\ \psi_2(\cdot) \end{bmatrix} = \begin{bmatrix} f_1(x) \\ f_2(x) \end{bmatrix} + (B(x) - B_0) \begin{bmatrix} u_1 \\ u_2 \end{bmatrix} \quad (25)$$

with the constant control gain matrix B_0 being given by

$$B_0 = \begin{bmatrix} b_{11} & 0 \\ 0 & b_{22} \end{bmatrix} \quad (26)$$

where b_{11} and b_{22} represent constant control gains. Here, matrix B_0 is chosen in the diagonal form so as to fully decouple the control of d-axis current and mechanical rotation speed.

Therefore, tracking error dynamics (19) can be rewritten in terms of perturbation by

$$\begin{bmatrix} \dot{e}_1 \\ \ddot{e}_2 \end{bmatrix} = \begin{bmatrix} \psi_1(\cdot) \\ \psi_2(\cdot) \end{bmatrix} + B_0 \begin{bmatrix} u_1 \\ u_2 \end{bmatrix} - \begin{bmatrix} \dot{i}_d^* \\ \ddot{\omega}_m^* \end{bmatrix} \quad (27)$$

A second-order high-gain perturbation observer (HGPO) is employed to estimate perturbation $\psi_1(\cdot)$ as

$$\begin{cases} \dot{\hat{i}}_d = \hat{\psi}_1(\cdot) + \dfrac{\alpha_{11}}{\epsilon_1}(i_d - \hat{i}_d) + b_{11}u_1 \\ \dot{\hat{\psi}}_1(\cdot) = \dfrac{\alpha_{12}}{\epsilon_1^2}(i_d - \hat{i}_d) \end{cases} \quad (28)$$

where Luenberger observer gains α_{11} and α_{12} are all positive constants, with $0 \leq \epsilon_1 \leq 1$.

Meanwhile, a third-order HGSPO is employed to estimate perturbation $\psi_2(\cdot)$ as

$$\begin{cases} \dot{\hat{\omega}}_m = \hat{\omega}_m + \dfrac{\alpha_{21}}{\epsilon_2}(\omega_m - \hat{\omega}_m) \\ \dot{\hat{\omega}}_m = \hat{\psi}_2(\cdot) + \dfrac{\alpha_{22}}{\epsilon_2^2}(\omega_m - \hat{\omega}_m) + b_{22}u_2 \\ \dot{\hat{\psi}}_2(\cdot) = \dfrac{\alpha_{23}}{\epsilon_2^3}(\omega_m - \hat{\omega}_m) \end{cases} \quad (29)$$

where observer gains α_{21}, α_{22}, and α_{23} are all positive constants, with $0 \leq \epsilon_2 \leq 1$.

The PERPC for PMSG system (19) is designed as

$$\begin{bmatrix} u_1 \\ u_2 \end{bmatrix} = B_0^{-1} \begin{bmatrix} -\hat{\psi}_1(\cdot) - k_{11}(\hat{i}_d - i_d^*) + v_1 \\ -\hat{\psi}_2(\cdot) - k_{21}(\hat{\omega}_m - \omega_m^*) - k_{22}(\hat{\omega} - \dot{\omega}_m^*) + v_2 \end{bmatrix} \quad (30)$$

with

$$\begin{cases} v_1 = -\lambda_1(i_d - i_d^*) \\ v_2 = -\lambda_2(\omega_m - \omega_m^*) \end{cases} \quad (31)$$

where control gains k_{11}, k_{21} and k_{22} are selected to guarantee the closed-loop system is stable. The energy reshaping coefficients of additional inputs λ_1 and λ_2 are chosen to inject extra system damping into the closed-loop system.

To this end, the overall control structure of PERPC (30) and (31) for PMSG system (19) is illustrated by Fig. 2. In particular, only the d-axis current i_d and mechanical rotation speed ω_m

needs to be measured. Finally, the calculated control inputs are modulated by the sinusoidal pulse width modulation (SPWM) technique [19].
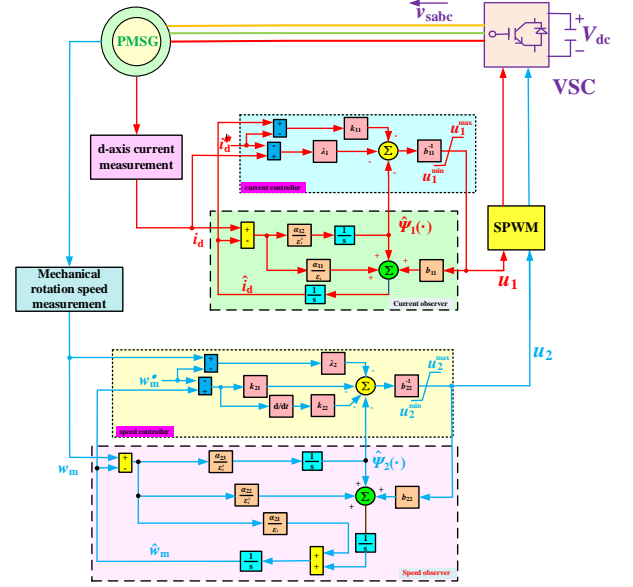

Fig.2. Overall PERPC structure of PMSG for MPPT.

5. CASE STUDIES

The proposed PERPC is applied on PMSG for MPPT, which control performance is compared to that of VC [7] and FLC [21], under three scenarios, e.g., (i) Step change of wind speed; (ii) Random wind speed variation; and (iii) Generator parameter uncertainties. Consider the control inputs may exceed the admissible capacity of VSC at some operation points, hence their values must be limited, i.e., $u_1 \in [-0.25, 0.25]$ per unit (p.u.) and $u_2 \in [-0.85, 0.85]$ p.u.. Furthermore, the PMSG system parameters and PERPC parameters are tabulated in Table 1 and Table 2, respectively.

Table 1. The PMSG system parameters

| PMSG rated power	P_{base}	2 MW	Field flux	K_e	136.25 V·s/rad
Radius of wind turbine	R	39 m	Pole pairs	p	11
d-axis stator inductance	L_d	5.5 mH	Air density	ρ	1.205 kg/m³
q-axis stator inductance	L_q	3.75 mH	Rated wind speed	v_{wind}	12 m/s
Total inertia	J_{tot}	10000 kg·m²	Stator resistance	R_s	50 $\mu\Omega$

Table 2. The control parameters of PERPC

Mechanical rotation speed control loop	$b_{11} = -1500$	$\alpha_{11} = 40$	$\alpha_{12} = 400$	$\epsilon_1 = 0.1$
	$k_{11} = 20$	$\lambda_1 = 15$		
d-axis current control loop	$b_{22} = -800$	$\alpha_{21} = 30$	$\alpha_{22} = 300$	$\alpha_{23} = 1000$
	$k_{21} = 25$	$k_{22} = 100$	$\lambda_2 = 20$	$\epsilon_2 = 0.1$

5.1. Step change of wind speed

Four consecutive step changes of wind speed are simulated which mimics a series of gust, while a step change of d-axis current is also applied. The system responses are depicted in Fig. 3. One can

find that PERPC can extract the maximum power from wind as its power coefficient remains closest to the optimum value. In contrast, VC performance degrades at different wind speed as its control parameters are determined by one-point linearization. Moreover, the d-axis current is fully decoupled from mechanical rotational speed and PERPC can regulate the d-axis current at the fastest rate without any overshoot.
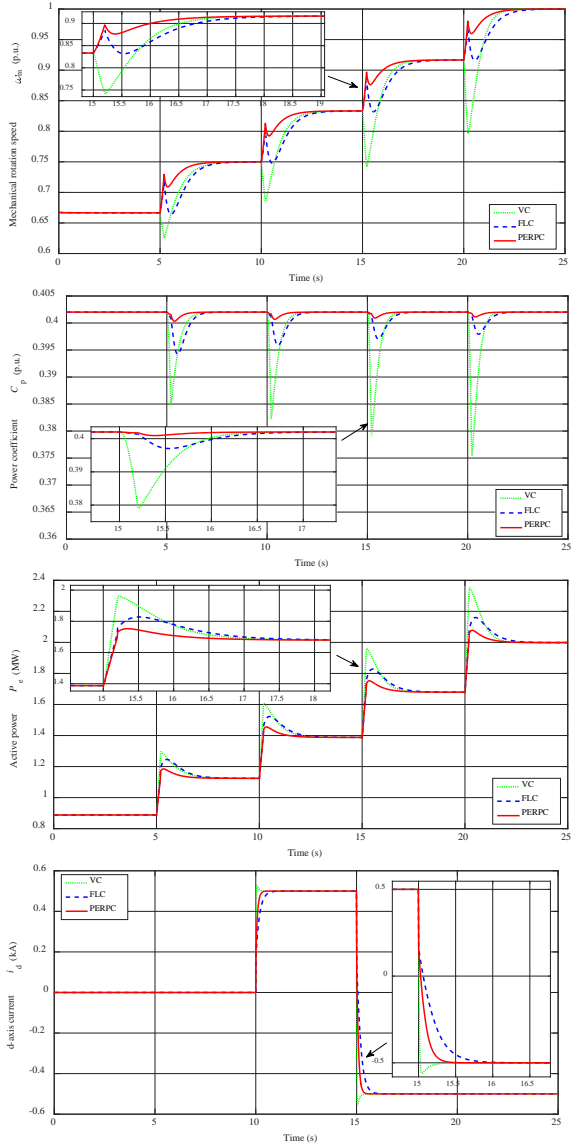
Fig. 3. System responses obtained under a series of step changes of wind speed.

5.2. Random wind speed variation

A random wind speed variation is applied to test the control performance of each controller, the obtained results are shown in Fig. 4. It is clear that PERPC outperforms other approaches in terms of the fastest optimal power tracking thanks to the real-time perturbation compensation and damping injection.
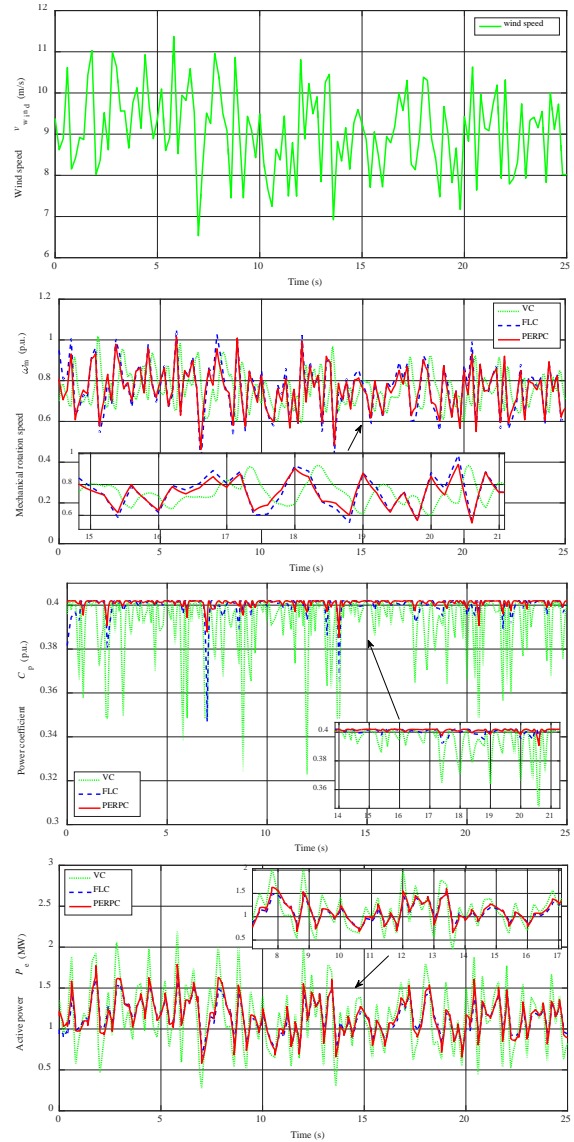
Fig. 4. System responses obtained under random wind speed variation.

5.3. Generator parameter uncertainties

In order to evaluate the robustness of each approach against to generator parameter uncertainties, a series of plant-model mismatches of stator resistance R_s and d-axis inductance L_d with ±20% variation around their nominal value are undertaken, in which a 1 m/s step increase of wind speed from the rated value (12 m/s) is applied and the absolute peak value of active power $|P_e|$ is recorded. Fig. 5 demonstrates that the variation of $|P_e|$ obtained by VC, FLC and PERPC is 15.9%, 26.1%, 11.6%, respectively. One can find that PERPC offers the greatest robustness in the presence of generator parameter uncertainties among all approaches thanks to the real-time perturbation compensation.
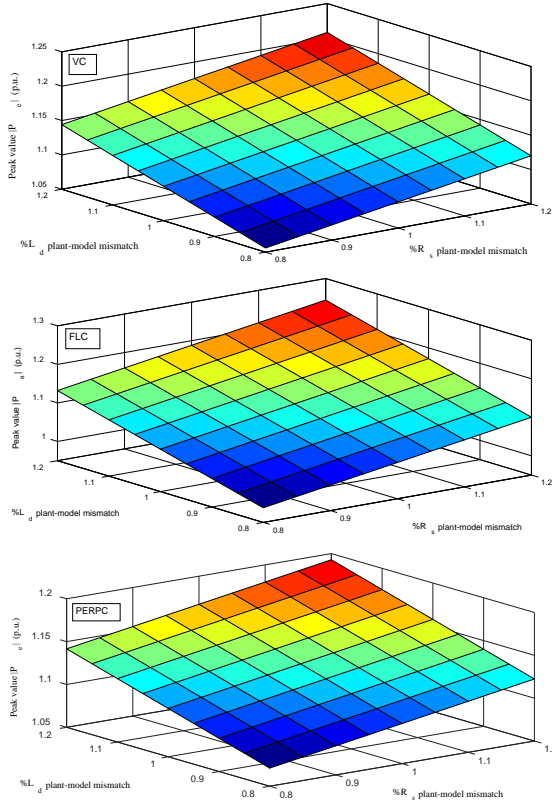
Fig. 5. Peak value of active power $|P_e|$ obtained under a 1 m/s step increase of wind speed from the rated value (12 m/s) with 20% variation of the stator resistance R_s and d-axis inductance L_d of three approaches, respectively.

5.4. Comparative studies

The integral of absolute error (IAE) indices of each controller required in each cases are provided in Table 3, where $\text{IAE}_x = \int_0^T |x - x^*|\, dt$. The simulation time T=25 s. From Table 3, it can be observed that PERPC owns the lowest IAE indices of mechanical rotation speed and d-axis current (in bold) in all cases.

Table 3. IAE indices of different controllers obtained in different cases (p.u.)

Case	Step change of wind speed	Random wind speed variation	Generator parameter uncertainties
Controller	IAE index IAE_{ω_m} of mechanical rotation speed		
VC	1.53E-01	6.52E-01	4.07E-02
FLC	1.28E-01	5.88E-01	3.41E-02
PERPC	**6.14E-02**	**2.96E-01**	**1.54E-02**
Controller	IAE index IAE_{id} of d-axis current		
VC	1.74E-02	7.05E-03	5.11E-03
FLC	1.46E-02	4.12E-03	4.35E-03
PERPC	**8.27E-03**	**2.11E-03**	**1.27E-03**

Table 4. The overall control costs(p.u.)

Case / Controller	Step change of wind Speed	Random wind speed variation	Generator parameter uncertainties
VC	0.268	0.697	0.089
FLC	0.196	0.466	0.075
PERPC	**0.153**	**0.359**	**0.049**

At last, the overall control costs of obtained in three cases are tabulated in Table 3. As shown in Table 4, PERPC just requires the minimal control costs in all three cases (in bold), hence it can provide the best control performance compared to that of VC and FLC.

6. CONCLUSION

The main novelty and contribution of this paper can be summarized as the following three aspects:

(1) An HGSPO is used to estimate the aggregated effect of PMSG nonlinearities, parameter uncertainties, and unmodelled dynamics, which is then fully compensated in the real-time by a passive controller. Hence, PERPC can effectively deal with various uncertainties;

(2) An extra system damping is injected into PMSG system to improve transient dynamics via energy reshaping, which can provide an improved MPPT performance under various wind profiles;

(3) PERPC does not require an accurate PMSG model while only the measurement of mechanical rotation speed and d-axis current is required. Hence, PERPC is quite easy to be implemented in practice.

References

[1] Yang, B.; Yu, T.; Shu, H.C.; Dong, J.; Jiang, L. Robust sliding-mode control of wind energy conversion systems for optimal power extraction via nonlinear perturbation observers, *Applied Energy*. http://dx.doi.org/10.1016/j.apenergy.2017.08.027.

[2] Yang, B.; Zhang, X.S.; Yu, T.; Shu, H.C.; Fang, Z.H. Grouped grey wolf optimizer for maximum power point tracking of doubly-fed induction generator based wind turbine. *Energy Conversion and Management* **2017**, 133, 427-443.

[3] Yang, B.; Hu, Y.L.; Huang, H.Y.; Shu, H.C.; Yu, T.; Jiang, L. Perturbation estimation based robust state feedback control for grid connected DFIG wind energy conversion system, *International Journal of Hydrogen Energy* **2017**, 42(33), 20994-21005.

[4] Yao, J.; Yu, M.; Gao, W.; Zeng, X. Frequency regulation control strategy for PMSG wind-power generation system with flywheel

energy storage unit. *IET Renewable Power Generation* **2017**, 11(8):1082-1093.

[5] Shehata, E.G. A comparative study of current control schemes for a direct-driven PMSG wind energy generation system. *Electric Power Systems Research* **2017**, *143*, 197-205.

[6] Youcef, S.; Sami, K.; Mohcene, B. Feedback linearization control based particle swarm optimization for maximum power point tracking of wind turbine equipped by PMSG connected to the grid. *International Journal of Hydrogen Energy* **2016**, 41, 20950-20955.

[7] Seyed, M.M.; Maarouf, S.; Hani, V.; Handy, F.B.; Mohsen, S. Sliding mode control of PMSG wind turbine based on enhanced exponential reaching law. IEEE Transactions on Industrial Electronics **2016**, 63(10), 6148-6159.

[8] Riad, A.; Toufik, R.; Djamila, R.; Abdelmounaim, T. Application of nonlinear predictive control for charging the battery using wind energy with permanent magnet synchronous generator. International Journal of Hydrogen Energy **2016**, 41, 20964-20973.

[9] Ikram, M.H.; Mohamed, W.N.; Najiba, M.B. Predictive control strategies for wind turbine system based on permanent magnet synchronous generator. *ISA Transactions* **2016**, 62, 73-80.

[10] Fantino, R.; Solsona, J.; Busada, C. Nonlinear observer-based control for PMSG wind turbine. *Energy* **2016***, 113, 248-257.

[11] Li, S.Q.; Zhang, K.Z.; Li, J.; Liu, C. On the rejection of internal and external disturbances in a wind energy conversion system with direct-driven PMSG. *ISA Transactions* **2016**, 61, 95-103.

[12] Ortega, R.; Schaft, A.; Mareels, I.; Maschke, B. Putting energy back in control. IEEE Control Systems **2001**, 21(2), 18-33.

[13] Santos, G.V.; Cupertino, A.F.; Mendes, V.F.; Seleme, S.I. Interconnection and damping assignment passivity-based control of a PMSG based wind turbine for maximum power tracking. 2015 IEEE 24th International Symposium on Industrial Electronics (ISIE), Buzios, **2015**, 306-311.

[14] Fernando, M.D.; Ortega, R. Adaptive passivity-based control for maximum power extraction of stand-alone windmill systems. Control Engineering Practice **2012**, 20, 173-181.

[15] Yang, B.; Jiang, L.; Yao, W.; Wu, Q.H. Perturbation observer based adaptive passive control for damping improvement of VSC-MTDC systems. Transactions of the Institute of Measurement and Control **2017**, 39(9), 1409-1420.

[16] Yang, B.; Jiang, L.; Yao, W.; Wu, Q.H. Perturbation estimation based coordinated adaptive passive control for multimachine power systems. Control Engineering Practice **2015**, 44, 172-192, 2015.

[17] Chen, J.; Jiang, L.; Yao, W.; Wu, Q.H. A feedback linearization control strategy for maximum power point tracking of a PMSG based wind turbine. *International Conference on Renewable Energy Research and Applications*, Madrid, Spain, 20-23 October **2013**, 79-84.

[18] Uehara, A.; Pratap, A.; Goya, T.; Senjyu, T.; Yona, A.; Urasaki, N.; Funabashi, T. A coordinated control method to smooth wind power fluctuations of a PMSG-based WECS. *IEEE Transactions on Energy Conversion.* **2011**, 26(6), 550-558.

[19] Wu, F.J.; Sun, D.Y.; Duan, J.D. Diagnosis of single-phase open-line fault in three-phase PWM rectifier with LCL filter. IET Generation Transmission & Distribution 2016, 10(6), 1410-1421.